Tetrahedron 66 (2010) 7204–7212

Contents lists available at ScienceDirect

Tetrahedron

journal homepage: www.elsevier.com/locate/tet

Pyrimidine based carboxylic acid terminated aromatic and semiaromatic hyperbranched polyamide-esters: synthesis and characterization

Saima Shabbir [a], Sonia Zulfiqar [a], Zahoor Ahmad [b], Muhammad Ilyas Sarwar [a,*]

[a] Department of Chemistry, Quaid-i-Azam University, Islamabad 45320, Pakistan
[b] Department of Chemistry, Faculty of Science, Kuwait University, PO Box 5969, Safat 13060, Kuwait

ARTICLE INFO

Article history:
Received 20 November 2009
Received in revised form 4 May 2010
Accepted 24 June 2010
Available online 19 July 2010

Keywords:
Hyperbranched polyamide-ester
Pyrimidine
Synthesis
Characterization

ABSTRACT

Carboxylic acid terminated aromatic and semiaromatic hyperbranched polyamide-esters (HBPAEs) containing pyrimidine moieties were prepared by polycondensation of 4-hydroxy-2,6-diaminopyrimidine (**CBB′**) to a double molar ratio of various diacid chlorides (**A_2**) without any catalyst. The products were soluble in organic solvents, such as *N*,*N*-dimethylformamide, *N*-methyl-2-pyrrolidone and displayed glass transition temperature (T_g) between 180 and 244 °C. The polymerization products have been investigated with FTIR, ^{1}H and ^{13}C NMR analyses and the degree of branching was higher than 60%. Amorphous polymers had inherent viscosity (η_{inh}) ranging between 0.21–0.28 dL/g and had excellent thermal stability with 10% weight loss at 346–508 °C.

1. Introduction

The interest in hyperbranched polymers (HBPs) increased rapidly over the past decade due to their unique physical and chemical properties as compared to their linear analogues.[1–13] HBPs were prepared mainly by polycondensation of an **AB_x** type monomer, which has one '**A**' functional group and *x* '**B**' functional groups.[14] This approach was widely used to synthesize a variety of HBPs, such as polyethers,[15] polyesters,[16] polyamides,[17] polyurethanes, [18] and so forth. Since, most of **AB_x** type monomers are unavailable commercially and synthesis of a new **AB_x** monomer is cumbersome. Therefore, the approaches via the polymerization of multifunctional monomers with equal reactivity were developed, however, **A_2**+**B_x**, must be performed under stringent conditions to avoid gelation, such as very low monomer concentrations, strictly controlled feed molar ratios, slow monomer addition rates and low monomer conversions.[19–21] Nevertheless, **A_2**+**B_x** approaches adopting monomers of suitable unequal reactivity have been demonstrated to be practical to prepare HBPs from commercially available monomers in one-pot processes.[22–26] These monomers with unequal reactivity can be **B_x** type monomers with **B** of different reactivity [22–24] or **CB_x** type monomers.[25,26] Despite the numerous developments in the field of HBPs, the main challenge, however, lies in the development of facile synthetic strategies that permit to prepare HBPs on the basis of readily available commercial monomers. In this perspective, our recent effort has focused on the development of a facile synthetic approach to more families of HBPs. We found that the reactivity of three types of functionalities in a trifunctional monomer, 4-hydroxy-2,6-diaminopyrimidine (HDAP), is different in polymerization with diacid chlorides. Therefore, the intermediate with diacid chloride groups and a -hydroxyl group may form at the initial stage of the reaction. Further polycondensations of such intermediates would lead to HBPAEs without gelation, as shown in Scheme 1. So, HBPAEs with terminal carboxylic acid group were formed via **A_2C** type intermediate (Scheme 1), which is produced through the reaction of the more reactive **B** and **B′** groups with the double molar concentration of **A_2** monomer. The approach reported here would facilitate further optimization of HBPAEs for wide applications. Thus, copolymerization reaction of HDAP with terephthaloyl chloride (TPC), isophthaloyl chloride (IPC), resulted in two fully aromatic HBPAE **21** and HBPAE **22**, whereas two semi-aromatic HBPAE **23** and HBPAE **24** originated from sebacoyl chloride (SC), and adipoyl chloride (AC). Conversely to classical **A_2**+**CB_x** approach, in this case the molar ratio of **A_2** to **CBB′** equals 2:1 and no gelation occurs in solution polymerization where **A_2C** dimer is formed initially which can be considered as a new **A_2B** type of monomer. Further reaction among **A_2C** molecules resulted in the formation of HBPAEs. Contrary to the classical methods, the strategy reported here capitulated HBPAEs without gelation by unequal reactivity of **CBB′** monomer. In this context, **A_2** monomer was added in molar excess to **CBB′** monomer and during the progress of synthesis, excess

* Corresponding author. Tel.: +92 51 90642132; fax: +92 51 90642241; e-mail address: ilyassarwar@hotmail.com (M.I. Sarwar).

0040-4020/$ – see front matter © 2010 Elsevier Ltd. All rights reserved.
doi:10.1016/j.tet.2010.06.065

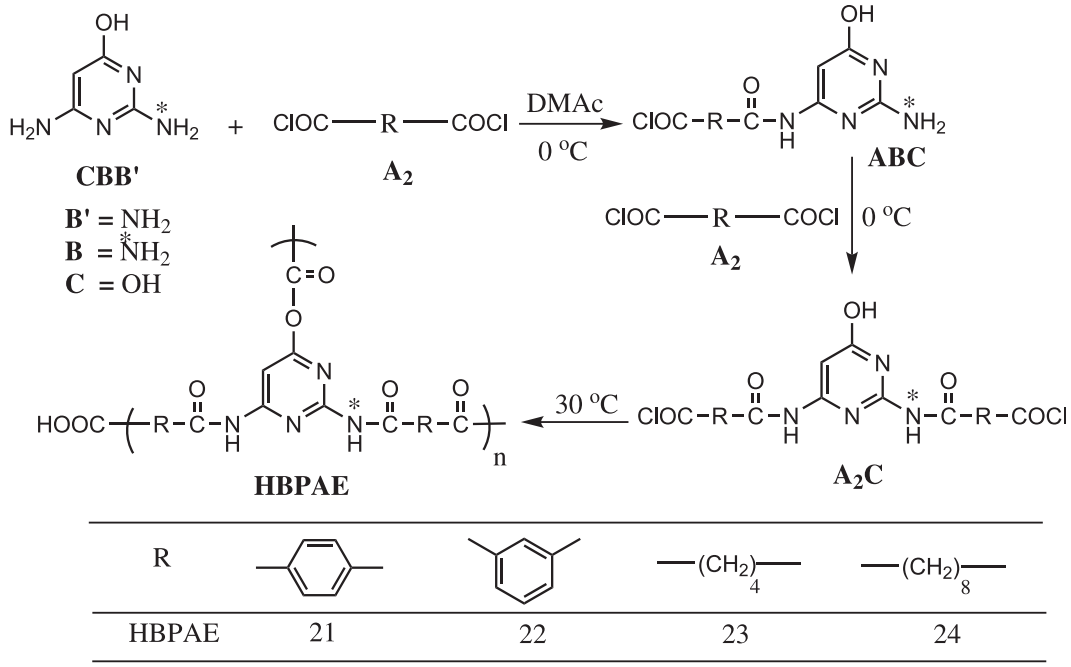

Scheme 1. Scheme for the synthesis of HBPAEs.

$\mathbf{A}_2$ monomer limited the molecular weight to increase so the risk of gel formation would be avoided. Compared to core-dilution method, the current synthetic stratagem was much simpler and it was hard to produce outgrowth. Moreover, compared with slow addition method, the present synthetic approach was more convenient and facilitated attaining HBPAEs without gelation. To the best of our knowledge there was no report regarding the synthesis of HBPAEs containing pyrimidine units through $2\mathbf{A}_2$+**CBB′** approach. Hence, the purpose of this article is to present our findings on synthesis of HBPAEs incorporating pyrimidine entities and its property profile in conjunction with the effect of introducing pyrimidine rings, as well as their structure property relationship. Therefore, HBPAEs were characterized in order to acquire a clear understanding of the influence exerted by structural variations in these polymers upon some of important properties, such as solubility, molar mass, T_g, η_{inh}, crystallinity, and thermal stability. The interest in these HBPAEs stems from the fact that heterocyclic pyrimidine units provide not only thermal stability, but also high electron affinity for materials useful in electronic applications.[27] Hence, this promising potential led to the synthesis of HBPAEs with the heterocyclic pyrimidine moiety. Additionally, intermolecular hydrogen bonding between pyrimidine nitrogens and the amide NHs of adjacent molecules provides the basis for material uniqueness. Quintessentially, pyrimidine moieties play a vital role in producing outstanding thermal facade of HBPAEs; therefore, pyrimidine rings influenced the structural and material characteristics of these HBPAEs.

2. Results and discussion

2.1. Polymer synthesis

Structure of the pyrimidine ring with both rigidity and polarizability was of interest. Thus, heteroaromatic monomer, containing the pyrimidine unit was exploited to prepare novel heteroaromatic HBPAEs with good thermostability and processability. Typically, the direct condensation of bisphenols and diacids cannot yield high molecular weight polyesters because of the strong leaving tendency of the phenylate moiety, so high molecular weight aromatic polyesters are prepared either by activated acid (acid chloride) or by acetylating or silylating the phenolic function. This means that HBPAEs with moderately high molecular weight can be obtained via the elaborate selection of monomers and optimization of reaction conditions. Accordingly, in current approach, HBPAEs were prepared based on **CBB′** type monomer (HDAP) and series of $\mathbf{A}_2$ type diacid chloride monomers (TPC, IPC, AC, and SC) as starting materials. The lower reactivity of amine at 2 position as compared with amine at 6 position was already demonstrated by ^{1}H NMR.[24] Due to electronegative nitrogen atoms in pyrimidine ring amine group at 2 position is less reactive than amine group at 6 position due to electron withdrawing inductive effect of heteroatom (N). Consequently, this method benefits from the fact that 2-amine group had a lower reactivity than the 6-amine group in HDAP, so, no gelation was observed during the polymerization probably due to the different reactivities of amine groups at 2 and 6 positions. Besides, it is also known that nucleophilic reactivity of amine group is much greater than that of hydroxyl group.[28] Hence, for this trifunctional monomer with less steric hindrance for amine at 6 position,[24] the reactivity sequence of different groups is as follows; 6 amine (**B′**)> 2 amine (**B**)>4 OH (**C**). It is reasonable to speculate that the polymerization of $2\mathbf{A}_2$+**CBB′** can be described by Scheme 1 on account of the reactivity sequence of **CBB′** monomer. Initially, amine at 6 position would react with $\mathbf{A}_2$ at 0 °C, forming **ABC** type precursor, then the residual $\mathbf{A}_2$ would react with amine on 2 position at the aforementioned temperature, producing $\mathbf{A}_2\mathbf{C}$ type intermediate and finally HBPAEs were obtained from polymerization of in situ formed $\mathbf{A}_2\mathbf{C}$ type intermediate at 30 °C. No gelation occurred through this polymerization process. The formation of $\mathbf{A}_2\mathbf{C}$ type intermediate was verified by the synthesis and isolation of $\mathbf{A}_2\mathbf{C}$ intermediate, which was subsequently characterized by CHN, FTIR, ^{1}H, and ^{13}C NMR techniques. These characterizations demonstrated that chemical composition of $\mathbf{A}_2\mathbf{C}$ is consistent with the proposed structure. Furthermore, data from elemental analysis was in good agreement with the calculated values. According to the mechanism described in Scheme 1, HBPAEs obtained may

contain focal units as those from normal $\mathbf{AB_2}$ type monomers. Therefore, HBPAEs with carboxylic acid terminal groups were prepared by performing polymerization of $2\mathbf{A_2}+\mathbf{CBB}'$ in DMAc. The first reaction was amidation (formation of amide linkage) producing an $\mathbf{A_2C}$ unit (with two acid chloride (**A**) groups and one alcohol (**C**) group). The following reaction was esterification giving rise to hyperbranched structures, which indicated that carboxyl chloride had mostly reacted with alcohol groups, and $\mathbf{A_2C}$ units had esterified to ensuing hyperbranched structures. So temperature of reaction mixture was gradually raised to 30 °C and kept there for 6 h to finish the esterification. Owing to the existence of an amount of reactive terminal acid chloride groups, cross-linking occurred easily in the purification processes of acid chloride terminated HBPAEs, so solid pure HBPAEs could not be obtained. Therefore, the terminal acid chloride groups were changed into stable carboxylic acid terminal groups by quenching with water. Structure elucidation of the synthesized HBPAEs was carried out by FTIR and NMR techniques. Figure 1 shows representative FTIR spectra of the HBPAEs. The broad band between 2500 and 3500 cm^{-1} were attributed to H-bonded amide N–H and acid O–H stretches. The strong and broad band between 3331–3325 cm^{-1} is chiefly attributed to O–H stretching of the H-bonded OH groups, which is the distinguishing feature of the COOH group. This broad band in the range of 3331–3325 cm^{-1} is also typical for the stretching of H-bonded O–H and N–H groups. The spectra of HBPAE **21**, **22**, **23**, and **24** showed bands around 3185–3012 cm^{-1} for aromatic C–H stretching. Amide C=O stretch was observed between 1642–1648 cm^{-1}. While carboxylic acid C=O and ester C=O bands appeared in the region of 1700–1687 and 1735–1725 cm^{-1}, respectively, confirming the structure. Moreover, IR spectra for HBPAE **23** and **24** displayed bands within the range of 2856–2948 cm^{-1} for aliphatic C–H stretching vibration. The bands at 1515, 1500 and, 1450 cm^{-1} are due to aromatic ring C=C stretching and bands at 1048–1056 and 1200–1242 cm^{-1} are due to the ester C–O stretching vibrations. All spectra are in compliance with the proposed structures. Based on the preceding results, analytical data indicated that HBPAEs contained carboxyl acid end groups, ester bonds and amide linkages, which are in conformity with objective polymers. Degree of branching was determined through ^{1}H NMR analysis as proton nuclei gave well separated peaks. The solubility of these HBPAEs in different solvents was evaluated. Thermal stability, T_g, η_{inh}, and crystallinity were examined using the corresponding techniques as described below.

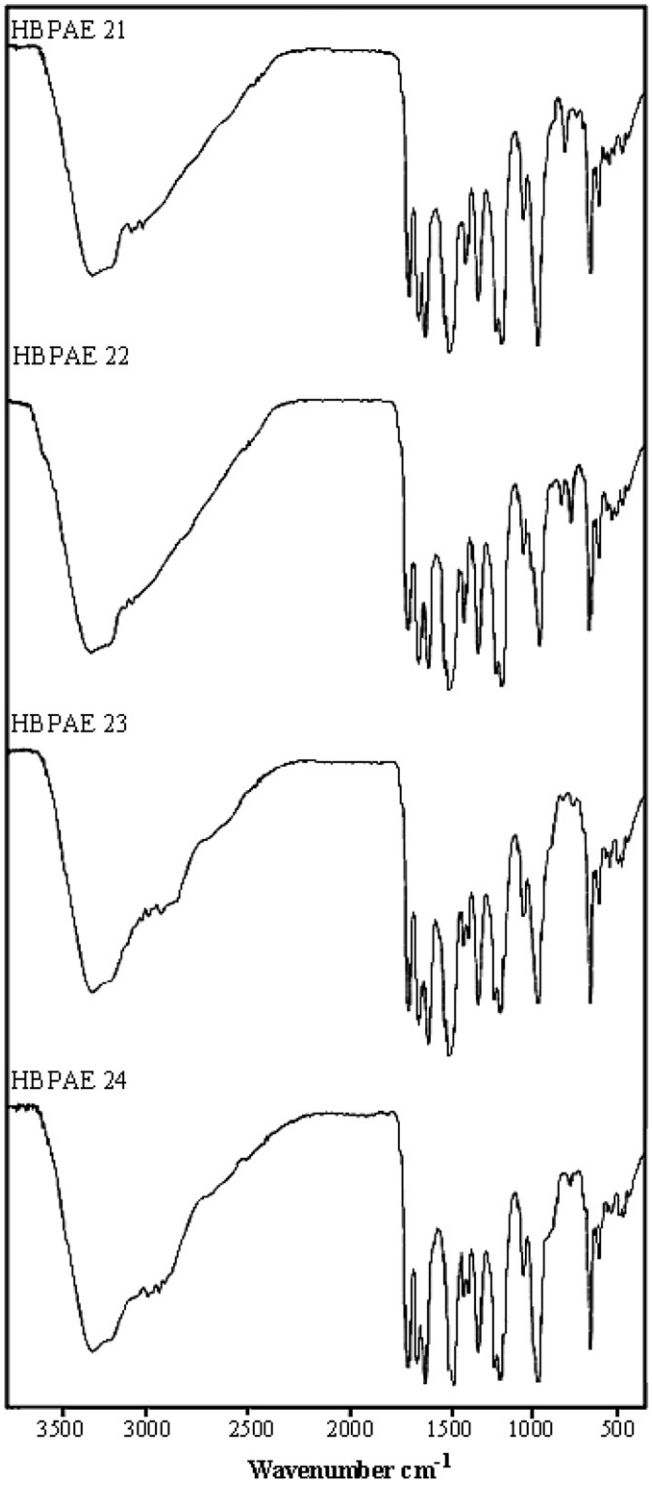

Figure 1. FTIR spectra of HBPAEs.

2.2. Degree of branching in HBPAEs

The degree of branching (DB) of HBPAEs can be evaluated by NMR spectroscopy, which was defined in the following equation: [29]

$$\mathrm{DB} = (\text{number of dendritic units} + \text{number of terminal units}/\text{number of total units})$$

Here DBs of HBPAEs should be assessed by taking the $\mathbf{A_2C}$ type intermediate as a starting monomer. Accordingly, $\mathbf{A_2C}$ type intermediate was synthesized, which, through a series of reactions, led to the formation of terminal, linear, and dendritic model compounds **1**, **2**, and **3**, respectively. In this way, the terminal, linear, and dendritic units were defined in Figure 2. Yet, the structural difference among the terminal, linear, and dendritic unit could be distinguished in ^{1}H NMR, so the DBs according to Fréchet's definition [29] were easy to be measured. In the ^{1}H NMR spectrum of HBPAEs, the resonance of the proton of the amide group appears in the range of 10.01–10.95 ppm, and a broad peak at 13.29–13.48 ppm from the proton of the terminal carboxylic acid group is also observed. Compared with the ^{1}H NMR spectra of the model compounds, the peaks of ^{1}H NMR spectra of the polymers were broader, including the carboxyl acid proton, due to the repeat units and the branched architecture of the polymers. The inbuilt property of HBPs is their broad molecular size distribution, which also led to significant peak broadening in ^{1}H NMR spectrum. The peak of carboxyl proton became broad and shifted downfield slightly (13.48, 13.40, 13.31, 13.29 ppm) because of intermolecular hydrogen bonding. There is prominent intermolecular H-bonding in amide

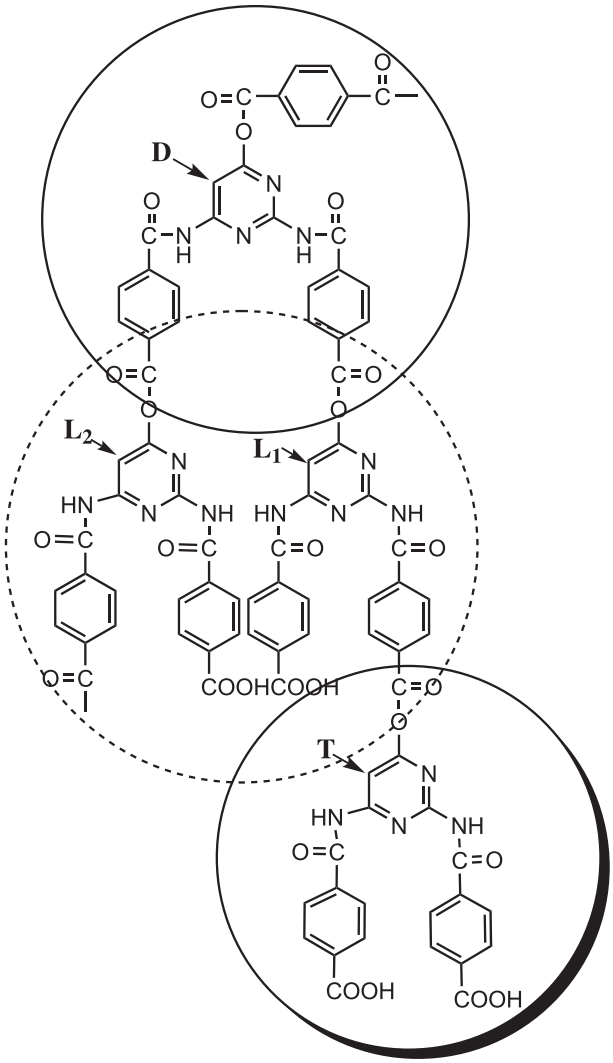

Figure 2. Structural repeat units of HBPAE **21**.

NH and nitrogen of pyrimidine (Scheme 2) group because of the abundant amide NH in the interior of the polymer molecule. Since H-bonding diminishes shielding, the NH signals move downfield while intermolecular H-bonding is enhanced. Although H-bonding

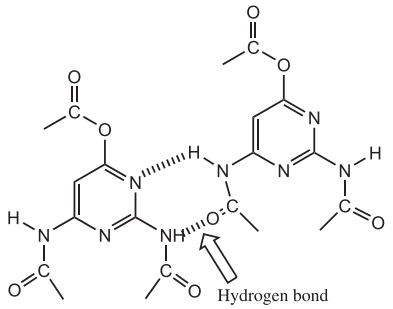

Scheme 2. Schematic representation of hydrogen bonding in HBPAEs.

exists between the COOH groups, it is much weaker than the amide group because amide groups lie in the interior of polymer along with pyrimidine units. The H-bonding is accompanied by exchange of H's from one molecule to another, resulting in signal broadening. For HBPAE **21**, the overall structure reveals four different types of subunits based on pyrimidine proton, thus, rendering pyrimidine unit as the criterion for the estimation of DB. These include one dendritic unit (D), which has no COOH group; two linear units (L_1 and L_2) with one COOH group and one terminal unit (T) with two COOH groups (Fig. 2). In some cases, it is also possible to identify the single focal unit A per molecule. But, as expected, the content of structural units with A function (one focal unit per molecule) is so small that it cannot be detected.[30] In addition, electro-deficient characteristic of pyrimidine ring causes broad COOH resonance peak in more downfield region (13.48 ppm). The amide proton region (10.01–10.95 ppm) is inappropriate for quantification due to concentration effects on chemical shifts and line widths. Since the chemical environment of proton in pyrimidine ring of D, L_1, L_2, and T units will be substantially different; the relative percentage of D, L_1, L_2, and T can be evaluated by ^{1}H NMR spectroscopy. To discriminate four subunits of the polymer backbone, model compounds **1**, **2**, and **3** were synthesized (Scheme 3) and used as the model compound for terminal, linear, and dendritic subunits, respectively. Comparison of the ^{1}H NMR spectra of these model compounds with ^{1}H NMR spectrum of HBPAE **1** allowed the resonance of D, L_1, L_2, and T subunits to be identified. Figure 3 shows the ^{1}H NMR spectra of model compounds **1**–**3**, and HBPAEs. Owing to structural uniqueness of pyrimidine moiety two types of linear subunits were identified in ^{1}H NMR spectrum of HBPAE **21** along with model compound **2**. Two distinct resonances for linear model compound **2**, were observed at 6.52 and 6.68 ppm while the corresponding proton for the dendritic model compound **3**, and terminal model compound **1**, appeared at 6.90 and 6.43 ppm, respectively. Multiplets in the region of 7–8 ppm belong to aromatic ring protons.

Whereas, in ^{1}H NMR spectrum of HBPAE **21** related protons were observed at 6.51–6.90 ppm. As compared with the ^{1}H NMR spectra of the model compounds, resonances at 6.62 and 6.80 ppm could be assigned to L_2 and L_1 subunits, while the resonances at 6.51 and 6.90 ppm could be assigned to the T and D subunits, respectively. Peak integration of resonances allowed the relative percentage of three subunits, dendritic (X_d), linear (X_{L1}, X_{L2}), and terminal unit (X_t) in HBPAE **21** and DB was evaluated. Therefore, on the basis of the ^{1}H NMR measurements, HBPAE **21** is a hyperbranched macromolecule with numerous terminal units and DB calculated by Fréchet's equation[29] was 0.67. Using the same analyzing strategy discussed above for the HBPAE **21**, DB values were evaluated to be 0.64, 0.62, and 0.61 for HBPAE **22**, **23**, and **24**, respectively (Table 1). Furthermore, since functional groups of monomers exhibit different reactivity, the degree of branching for HBPAEs is higher than 60%.

$$\text{Terminal} \xrightarrow{K_T} \text{Linear} \xrightarrow{K_L} \text{Dendritic}$$

When the rate of the formation of linear units is greater than rate of formation of terminal units ($k_L > k_T$), the amount of dendritic units would be increased during the polymerization of $\mathbf{AB}_x$ type monomers.[30] It was observed (Table 1) that X_L became larger than X_t thus leading to enhanced DB of HBPAEs.

2.3. Organosolubility

Normally, high solubility is a preferred requirement for processing polymers. All the carboxylic acid terminated HBPAEs had good solubility in DMSO and NMP. Effect of introducing rigid amide structure and heteroaromatic pyrimidine units in the backbone was strongly depicted in solubility besides thermal properties (Table 2). Enhanced solubility of HBPAEs could be endorsed to both nature of terminal functional groups and highly branched architecture. Nevertheless, inferior solubility relative to earlier HBPAEs [26] is due to the presence of pyrimidine structural units that aggravate macromolecule hydrogen bonding between amide NHs and pyrimidine

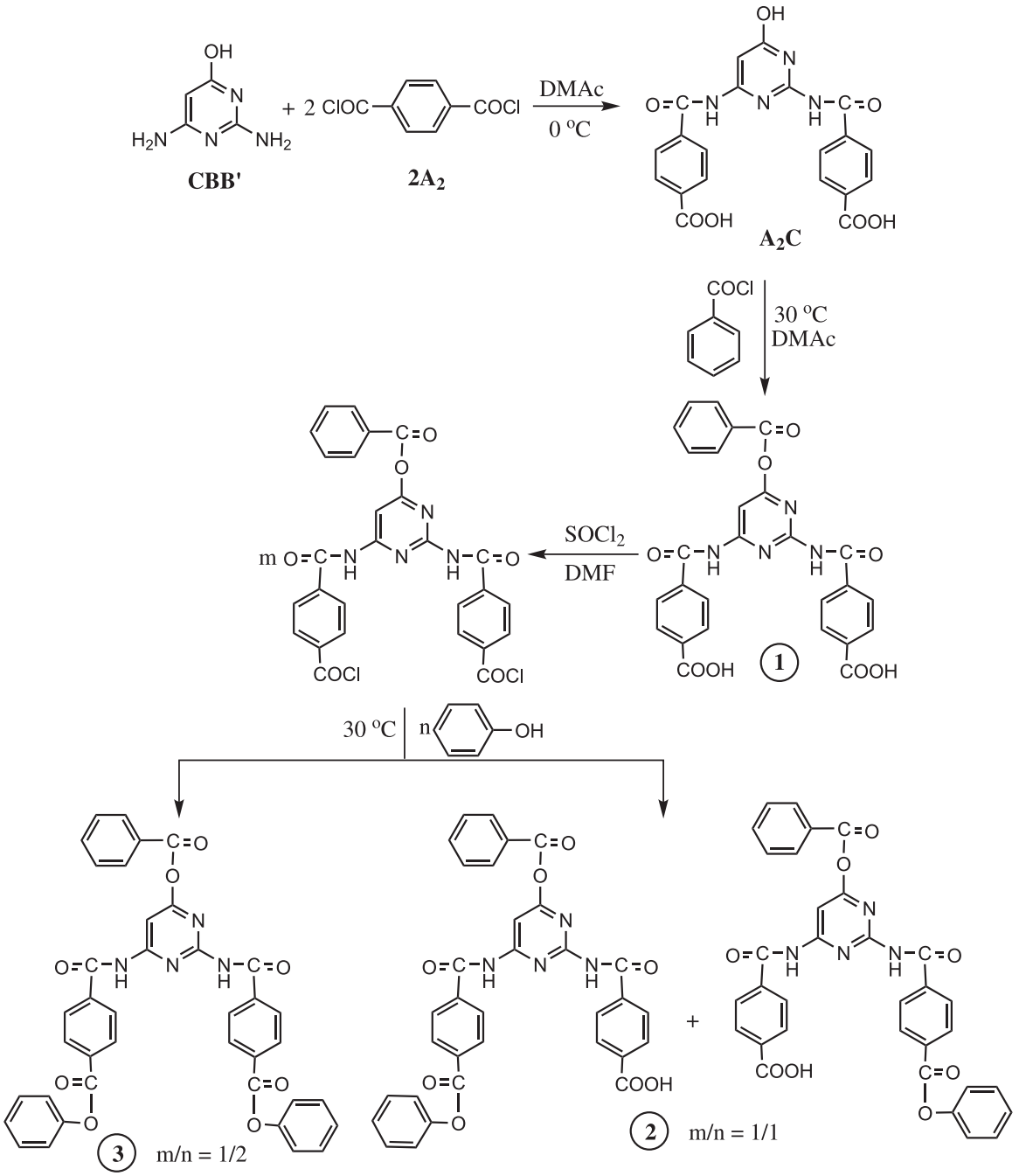

Scheme 3. Scheme for the synthesis of model compounds.

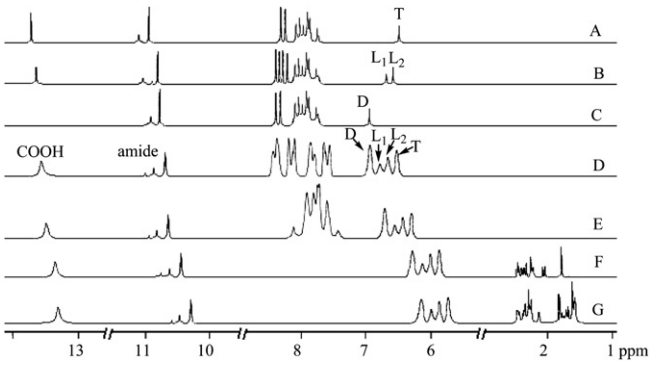

Figure 3. ^{1}H NMR spectra of A: model compound **1**; B: model compound **2**; C: model compound **3**; D: HBPAE **21**; E: HBPAE **22**; F: HBPAE **23**; G: HBPAE **24**.

Table 1
η_{inh}, M_w, and DB of HBPAEs in DMSO

Polymer	η_{inh}[a] (dL/g)	M_w[b]	PDI= M_w/M_n[b]	DB (Fréchet)[c]= $(X_d+X_t)/(X_d+X_t+X_{L1}+X_{L2})$	Unit fraction			
					[c]X_d	[c]X_{L1}	[c]X_{L2}	[c]X_t
HBPAE **21**	0.28	—	—	0.67	0.37	0.12	0.21	0.30
HBPAE **22**	0.25	—	—	0.64	0.35	0.13	0.23	0.29
HBPAE **23**	0.23	58,858	2.5	0.62	0.31	0.13	0.25	0.31
HBPAE **24**	0.21	41,954	2.2	0.61	0.30	0.14	0.25	0.31

[a] Measured in DMSO at a concentration of 0.5 g/dL at 30 °C.
[b] Determined by GPC based on polystyrene standards.
[c] X_d, dendritic unit fraction; X_{L1} and X_{L2}, linear unit fractions; X_t, terminal unit fraction. The four unit fractions are calculated from the integration of the deconvoluted peaks assigned to the central pyrimidine unit in the ^{1}H NMR spectra.

Table 2
Solubility[a] behavior of different HBPAEs

Polymer	Solvent[b]					
	NMP	DMAc	DMF	DMSO	THF	$CHCl_3$
HBPAE **21**	++	+−	+−	++	−	−
HBPAE **22**	++	+−	+−	++	−	−
HBPAE **23**	++	++	++	++	−	−
HBPAE **24**	++	++	++	++	−	−

[a] Solubility: ++ soluble at room temperature, +− partially soluble at room temperature, − insoluble.
[b] Scale: 15 mg/1 mL.

nitrogens. Figure 3 clearly demonstrates the existence of hydrogen bonding as deshielding via intermolecular hydrogen bonding caused COOH and NH signals to move downfield. Prominently the presence of alkyl groups in the semi-aromatic HBPAEs derived from aliphatic acid chlorides caused improvement of solubility in contrast to fully aromatic HBPAEs. In view of that, HBPAE **21** and **22**, derived from aromatic diacid chlorides with more rigid structure, exhibited lower solubility in various solvents.

2.4. Viscometry and molar mass

Low viscosity of HBPAEs relative to linear analogues was suggested to originate from their compact molecular nature, i.e., globular shape with less physical entanglement based on highly branched structure. However, η_{inh} of HBPAEs, 0.21–0.28 dL/g (Table 1), is comparable to hyperbranched polyester-amides reported by Liu et al.[31] indicating a moderate molecular weight. Their η_{inh} amplified with the increase of *p*-phenylene unit. This indicated that the polymer chain rigidity increased as a function of their *para* linkages (Table 1). On the contrary, η_{inh} decreased only slightly with the incorporation of flexible alkyl linkage in HBPAE **23** and **24**, when judged against HBPAE **21** and **22**. Table 1 also lists the M_w and polydispersity index (PDI) of the resultant HBPAE **23** and **24** by GPC analysis. It is previously established that this method has limited suitability for HBPs and usually undervalues the exact molar mass of HBPs due to their smaller hydrodynamic radii compared to linear analogues.[29] On the other hand, the interactions of the polar end group with solvent are stronger, which overrates the actual value of molecular weight. But for a HBP containing a long linear aliphatic chain, these two effects may decline and the determined mass may be close to the true value. Besides, the HBPAEs exhibited moderate molecular weights with broad molecular weight distributions due to the highly branched structure. The PDI were high, which was a typical result for $\mathbf{AB}_x$ polycondensation predicted by Flory.[1]

2.5. Thermal analyses

The thermal profile of HBPAEs was evaluated in N_2 at a heating rate of 10 °C/min using DSC and TGA techniques. Polymers showed T_gs ranging from 180 to 244 °C (Fig. 4) according to their DSC analysis (T_g was taken as the midpoint of the change in slope of the baseline). In the present investigation, COOH-terminated HBPAE **21** has a T_g of 244 °C and HBPAE **22**, **23**, and **24** was lower, 227, 207, and 180 °C, respectively (Table 3). HBPAE **23** and **24** exhibited much lower T_gs than HBPAE **21** and **22** due to the plasticization of the more flexible alkyl groups.

In addition, the higher T_g of HBPAEs compared to that of former HBPAEs [26] might be ascribed to the existence of heteroaromatic pyrimidine rings. Besides, thermal stabilities of HBPAEs were evaluated by thermogravimetric analysis (TGA) and initial decomposition temperature (T_0) ranged between 281–435 °C (Fig. 5). Temperatures for 10% gravimetric loss (T_{10}), significant for the

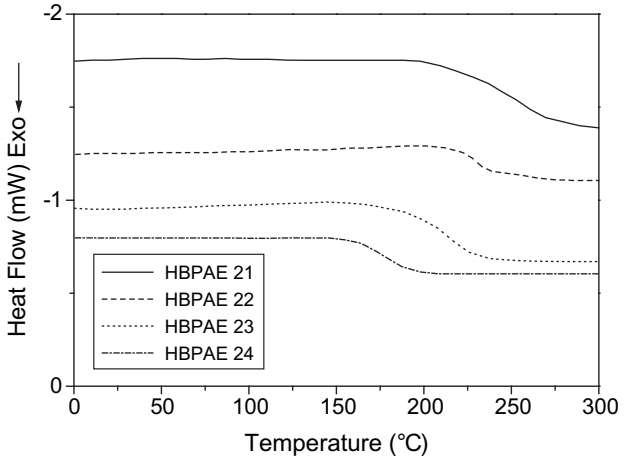

Figure 4. DSC thermograms of HBPAEs at heating rate of 10 °C/min in N_2.

Table 3
Thermal analysis data of different HBPAEs

Polymer	T_g (°C)[a]	T_0 (°C)[b]	T_{10} (°C)[c]	T_{max} (°C)[d]	Y_c at 600 °C (%)[e]
HBPAE **21**	244	435	508	583	71
HBPAE **22**	227	425	498	564	68
HBPAE **23**	207	318	364	543	55
HBPAE **24**	180	281	346	532	54

[a] T_g: Glass transition temperature.
[b] T_0: Initial decomposition temperature.
[c] T_{10}: Temperature for 10% weight loss.
[d] T_{max}: Maximum decomposition temperature.
[e] Y_c: Char yield; weight of polymer remained.

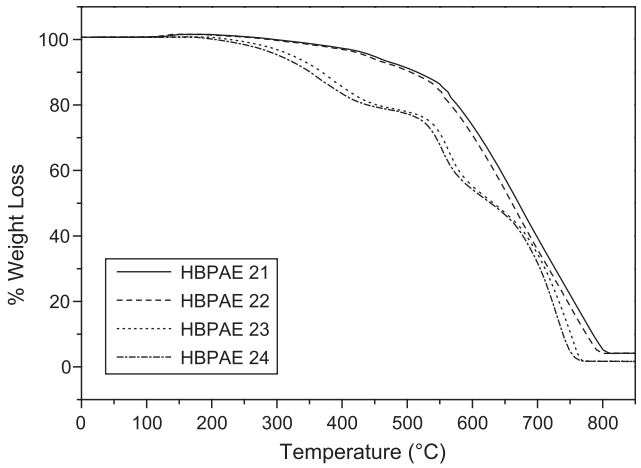

Figure 5. TGA curves of HBPAEs at heating rate of 10 °C/min in N_2.

evaluation of thermal stability, were in the range of 346–508 °C and also char yields at 600 °C were about 54–71%, which is indicative of good thermal stability. It was found that T_{10} of HBPAE **21** was slightly higher than that of HBPAE **22**, which may be attributed to the fact that the *meta*-oriented architecture have less dense polymer chain packing than *p*-oriented ones due to the smaller conformational entropy of *p*-oriented chain. Consequently, the former has better thermal stability than the latter.

According to the acquired results, these HBPAEs established high thermal stability that could be ascribed to the incorporation of heterocyclic pyrimidine moieties and pre-formed amide groups as well as the existence of intermolecular hydrogen bonding

between pyrimidine nitrogen and amide NH. Hence, all resulting HBPAEs are thermally stable owing to their aromatic heterocyclic structure.

2.6. X-ray diffraction

According to Figure 6, HBPAE **21** and **22** possess a slight degree of ordering with hydrogen bonding derived from amide and pyrimidine components exhibiting a minute crystalline pattern. However, there were no crystalline melting transitions (T_m) detected by DSC (Fig. 4). This probably indicated that either HBPAEs were predominately amorphous with only a low degree of molecular ordering, or that the T_m value of ensuing HBPAEs was higher than the measurement range used in DSC experiment. By and large, HBPs are identified not to crystallize and amorphous behavior recommended that the branched structure hindered crystallization. Finally, the amorphous character is also supported by the reasonable solubility of HBPAEs.

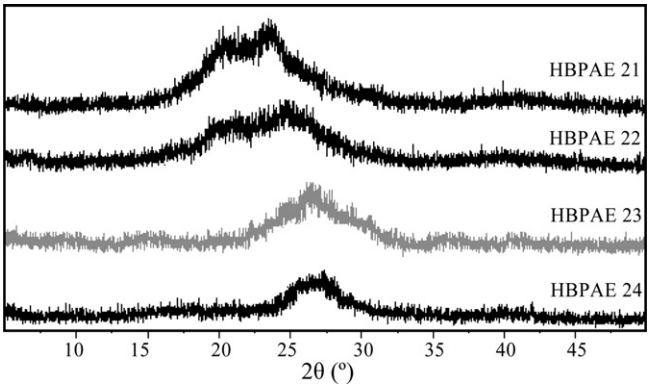

Figure 6. X-ray diffraction curve of HBPAEs.

3. Conclusions

On the basis of the reactivity sequence for **CBB′** type monomer in the polymerization with $\mathbf{A}_2$ monomers, $2\mathbf{A}_2$+**CBB′** approach to HBPAEs was set up. Pyrimidine containing HBPAEs with carboxylic acid terminal groups were obtained by polymerization of **CBB′** with a double molar $\mathbf{A}_2$ via $\mathbf{A}_2\mathbf{C}$ type intermediate that originated from its ABC type precursor when polymerization was performed in DMAc from 0 to 30 °C. HBPAEs obtained using a two-fold molar-excess of $\mathbf{A}_2$ were characterized by FTIR and ^{1}H NMR spectroscopy and had η_{inh} between 0.21–0.28 dL/g. Thermal behavior of these soluble HBPAEs was studied by TGA exhibiting ample thermal stability owing to amide linkages and pyrimidine groups. The degree of branching determined by ^{1}H NMR ranged between 0.67 and 0.61. DSC served to envisage T_g of amorphous polymers sited between 180 and 244 °C. Introduction of pyrimidine ring with rigidity and aromaticity, as well as, the contribution of polarizability resulting from nitrogen atom in pyrimidine ring has been substantiated. Prospective utilizations of these HBPAEs include reactive COOH chain ends that remain after polymerization, which present sites that can be employed for surface or bulk modification.

4. Experimental

4.1. Measurements

IR spectra of monomer and polymers were monitored at a resolution of 4 cm^{-1}, using Excalibur Series FTIR Spectrometer, Model No. FTSW 300 MX manufactured by BIO-RAD. NMR spectrum was recorded at room temperature using BRUKER Spectrometer operating at 300.13 MHz for ^{1}H NMR spectra. Solvent used was deuterated dimethyl sulfoxide (DMSO-d_6). Elemental analysis was performed using a Perkin–Elmer 2400 CHN elemental analyzer. Inherent viscosity ($\eta_{inh}=\ln\eta_r/c$) was measured in DMSO at 30 °C with an Ubbelohde viscometer on polymer solutions with a concentration of 0.5 g/dL. Qualitative solubility was determined with 15 mg of polymer in 1 mL of various solvents at room temperature. Gel permeation chromatography (GPC) was performed in DMF containing 0.01 mol/L of lithium bromide as an eluent. The absolute molecular weight was calculated by GPC with a light scattering detector. Thermal stability of the polymers was determined by METTLER TOLEDO TGA/SDTA 851^e thermogravimetric analyzer using 1–5 mg of the sample in an Al_2O_3 crucible heated from 25 to 900 °C at a heating rate of 10 °C/min under nitrogen atmosphere with a gas flow rate of 30 ml/min. In order to obtain glass transition temperature, differential scanning calorimetry (DSC) was performed by a METTLER TOLEDO DSC 822^e differential scanning calorimeter, using 5–10 mg of samples encapsulated in aluminum pans and heated at a rate of 10 °C/min under nitrogen atmosphere. X-ray diffraction pattern was performed at room temperature on an X-ray diffractometer (3040/60 X'pert PRO) using Ni-filtered Cu Kα radiation (40 kV, 30 mA) with scanning rate of 0.04°/s.

4.2. Materials

4-Hydroxy-2,6-diaminopyrimidine (HDAP), benzoyl chloride, TPC, IPC, SC, and AC were procured from Aldrich and used as received. *N*-Methyl-2-pyrrolidone (NMP), dimethyl sulfoxide (DMSO), and thionyl chloride ($SOCl_2$) were obtained from Merck and used as received. *N*,*N*-Dimethylacetamide (DMAc), methanol, *N*,*N*-dimethylformamide (DMF), and tetrahydrofuran (THF) were received from Aldrich and distilled prior to use.

4.3. Hyperbranched polyamide-esters synthesis

The synthesis of HBPAE **21**, **22**, **23**, and **24** was carried out in a dry 250 mL four-necked round bottom flask equipped with a magnetic stirrer, a thermometer and a drying tube placed in a dry box. HDAP (10 mmol) was charged into the reaction flask, followed by the addition of 50 mL dry DMAc with continuous stirring. The reaction flask was placed in an ice-salt bath and cooled at 0 °C for 15 min. After complete dissolution, 20 mmol of the corresponding diacid chloride was added at once (Scheme 1). Stirring was continued for an additional 2 h at the above-mentioned temperature. Then the temperature of the reaction mixture was allowed to rise gradually to 30 °C and further agitated for 6 h. The homogeneous reaction was maintained at 30 °C for 24 h. Water (10 mL) was subsequently added to quench the residual acid chloride and the heterogeneous solution was stirred for 30 min. A stoichiometric amount of TEA was added to remove HCl produced during the polymerization reaction otherwise it would act as an impurity that might yield a low molecular weight polymer. The solution was centrifuged to isolate the precipitates from the neat HBPAEs. Finally, the polymer solution was slowly poured into methanol with uniform stirring upon which precipitates of HBPAE immediately formed. The polymer was isolated by filtration, washed successively with methanol and water. Polymer samples were purified by repeated precipitation from their solutions in DMAc using methanol as non-solvent. The precipitated polymers were isolated, washed and dried under vacuum at 80 °C for 24 h. Yield: 4.52 g pale yellow powder, 85%; *HBPAE* **21**; IR (KBr) ν_{max}: 3300–2500 (N–H, OH), 3012, 3165 (Ar C–H), 1735 (ester C=O), 1700 (acid C=O), 1648 (amide C=O), 1515, 1450 (Ar C=C), 1321, 1242, 1202, 1050 (C–O), 812 (*p*-Ar), 502, 451. ^{1}H NMR (300 MHz, DMSO-d_6, ppm): δ 13.49 (br, COOH), 10.01–10.69 (m, amide NH), 8.32 (d,

J=9.3 Hz, *p*-Ar), 8.05 (d, J=9.1 Hz, *p*-Ar), 7.75 (d, J=9.2 Hz, *p*-Ar), 7.51 (d, J=9.0 Hz, *p*-Ar), 6.90 (s, pyrimidine), 6.81 (s, pyrimidine), 6.63 (s, pyrimidine), 6.51 (s, pyrimidine). ^{13}C NMR (75 MHz, DMSO-d_6, ppm): δ 176.82, 176.61, 176.36, 176.28 (acid C=O), 176.01, 175.84, 175.65, 175.43, 175.25, 175.04, 174.97 (ester C=O), 167.61, 167.35, 167.22, 167.08, 166.90, 166.74 (amide C=O), 163.51, 162.43, 160.51, 156.77, 152.68, 150.21, 142.76, 139.92, 135.26, 134.08, 130.75, 130.46, 129.53, 128.52, 128.86, 127.89, 127.63, 125.96, 121.18, 98.39, 97.65, 96.47, 91.28. Yield: 4.58 g pale yellow powder, 86%; *HBPAE* **22**; IR (KBr): 3300–2500 (N–H, OH), 3046, 3185 (Ar C–H), 1730 (ester C=O), 1698 (acid C=O), 1648 (amide C=O), 1515, 1450 (Ar C=C), 1320, 1241, 1200, 1048 (C–O), 856, 798 (*m*-Ar), 502, 450. ^{1}H NMR (300 MHz, DMSO-d_6, ppm): δ 13.41 (br, COOH), 10.95–10.69 (m, amide NH), 7–8 (m, *m*-Ar), 6.69 (s, pyrimidine), 6.51 (s, pyrimidine), 6.40 (s, pyrimidine), 6.26 (s, pyrimidine). ^{13}C NMR (75 MHz, DMSO-d_6, ppm): δ 176.80, 176.58, 176.35, 176.29 (acid C=O), 175.97, 175.85, 175.67, 175.42, 175.21, 175.03, 174.96 (ester C=O), 167.60, 167.32, 167.21, 167.05, 166.89, 166.73 (amide C=O), 162.89, 161.25, 160.96, 158.08, 152.68, 151.36, 145.34, 136.50, 133.89, 130.54, 129.24, 128.75, 127.66, 127.57, 121.32, 98.42, 97.67, 96.53, 91.36. Yield: 4.13 g yellow powder, 84%; *HBPAE* **23**; IR (KBr): 3300–2500 (N–H, OH), 3125 (Ar C–H), 2925, 2856 (Ali C–H), 1728 (ester C=O), 1687 (acid C=O), 1645 (amide C=O), 1500, 1450 (Ar C=C), 1346, 1236, 1202, 1054 (C–O), 501, 452. ^{1}H NMR (300 MHz, DMSO-d_6, ppm): δ 13.31 (br, COOH), 10.85–10.44 (m, amide NH), 6.28 (s, pyrimidine), 6.11 (s, pyrimidine), 5.98 (s, pyrimidine), 5.84 (s, pyrimidine), 2.50–1.75 (m, CH_2). ^{13}C NMR (75 MHz, DMSO-d_6, ppm): δ 177.68, 177.53, 177.36, 177.23 (acid C=O), 176.96, 176.78, 176.64, 176.48, 176.32, 176.15, 175.97 (ester C=O), 168.54, 168.38, 168.23, 168.06, 1676.90, 167.72 (amide C=O), 160.47, 150.98, 145.79, 99.65, 98.29, 97.76, 92.42, 35.84, 33.42, 33.27, 32.96, 25.13, 24.50, 24.16. Yield: 5.20 g yellow powder, 86%; *HBPAE* **24**; IR (KBr): 3300–2500 (N–H, OH), 3126 (Ar C–H), 2948, 2876 (Ali C–H), 1725 (ester C=O), 1687 (acid C=O), 1642 (amide C=O), 1500, 1450 (Ar C=C), 1342, 1240, 1200, 1056 (C–O), 498, 446. ^{1}H NMR (300 MHz, DMSO-d_6, ppm): δ 13.29 (br, COOH), 10.60–10.31 (m, amide NH), 6.16 (s, pyrimidine), 6.01 (s, pyrimidine), 5.87 (s, pyrimidine), 5.81 (s, pyrimidine), 2.51–2.13 (m, CH_2), 1.89–1.47 (m, CH_2). ^{13}C NMR (75 MHz, DMSO-d_6, ppm): δ 177.69, 177.52, 177.38, 177.25 (acid C=O), 176.94, 176.81, 176.65, 176.50, 176.34, 176.14, 175.89 (ester C=O), 168.56, 168.37, 168.24, 168.05, 1676.92, 167.73 (amide C=O), 160.32, 150.92, 145.65, 99.72, 98.36, 97.84, 92.63, 36.22, 33.61, 29.43, 26.17, 29.06, 28.74, 25.78, 25.10.

4.3.1. Synthesis of $\mathbf{A_2C}$ *intermediate.* HDAP (0.126 g, 1.0 mmol) was dissolved in 5 mL of DMAc with continuous stirring under N_2 flow. To this solution TPC (0.406 g, 2.0 mmol) was added in DMAc (5 mL) in 30 min (Scheme 3). The reaction mixture was maintained at 0 °C for 2 h. Water (2 mL) was subsequently added and stirring was continued for 30 min. Finally, the precipitates of $\mathbf{A_2C}$ were isolated by filtration, washed with methanol and water in succession, and dried under vacuum at 80 °C for 24 h. Yield: 0.4012 g white powder, 95%; mp 346 °C; IR (KBr) ν_{max}: 3500–2500 (N–H, OH), 3028 (Ar C–H), 1700 (acid C=O), 1657 (amide C=O), 1606, 1515, 1450 (Ar C=C), 1236, 1202, 1038 (C–O), 832 (*p*-Ar), 502. ^{1}H NMR (300 MHz, DMSO-d_6, ppm): δ 13.65 (br, 2H, COOH), 10.86 (s, 1H, amide NH), 10.77 (s, 1H, amide NH), 9.14 (br, 1H, Ar OH), 8.16 (d, 4H, J=5.3 Hz, *p*-Ar), 8.31 (d, 4H, J=5.4 Hz, *p*-Ar), 6.45 (s, 1H, pyrimidine). ^{13}C NMR (75 MHz, DMSO-d_6, ppm): δ 173.68, 173.52 (acid C=O), 165.13, 164.98 (amide C=O), 160.62, 156.47, 148.98, 139.51, 133.40, 130.23, 127.21, 91.04. Anal. Calcd for $C_{20}H_{14}N_4O_7$: C, 56.88; H, 3.34; N, 13.27%. Found: C, 56.85; H, 3.31; N, 13.17%.

4.3.2. Synthesis of model compound ***1***. In a dried 100 mL three-neck flask, $\mathbf{A_2C}$ (0.422 g, 1.0 mmol) was dissolved in 5 mL of DMAc, the mixture was stirred under N_2 flow. To this solution was added benzoyl chloride (0.141 g, 1.0 mmol) in DMAc (5 mL) in 30 min (Scheme 3). The reaction mixture was maintained at 30 °C for 24 h. Water (2 mL) was subsequently added to quench the reaction and stirring was continued for 30 min. A stoichiometric amount of TEA was used as HCl scavenger. The solution obtained was poured into methanol and precipitates were washed with water and methanol successively, to furnish model compound **1** after drying in vacuum. Yield: 0.5054 g light yellow powder, 96%; mp 375–380 °C; IR (KBr) ν_{max}: 3300–2500 (N–H, OH), 3040 (Ar C–H), 1698 (acid C=O), 1654 (amide C=O), 1602, 1515, 1450 (Ar C=C), 1232, 1204, 1036 (C–O), 835 (*p*-Ar), 740, 710 (monosubst Ar), 501. ^{1}H NMR (300 MHz, DMSO-d_6, ppm): δ 13.65 (s, 2H, COOH), 11.03 (s, 1H, amide NH), 10.87 (s, 1H, amide NH), 8.22 (d, 4H, J=5.5 Hz, *p*-Ar), 8.34 (d, 4H, J=5.6 Hz, *p*-Ar), 7–8 (m, 5H, Ar), 6.44 (s, 1H, pyrimidine). ^{13}C NMR (75 MHz, DMSO-d_6, ppm): δ 176.75, 176.59 (acid C=O), 175.93 (ester C=O), 167.56, 167.30 (amide C=O), 162.46, 160.51, 156.73, 148.65, 139.91, 134.07, 133.86, 131.38, 130.45, 128.50, 127.54, 93.38. Anal. Calcd for $C_{27}H_{18}N_4O_8$: C, 61.60; H, 3.45; N, 10.64%. Found: C, 61.56; H, 3.40; N, 10.63%.

4.3.3. Synthesis of model compound ***2***. A sample of model compound **1** (0.00316 g, 0.006 mmol) was dissolved in anhydrous DMF and $SOCl_2$ (0.95 mL, 0.01 mmol) was added. A clear solution was obtained after about 10 min. The reaction mixture was refluxed for 6 h. The solvent and excess of $SOCl_2$ were removed by rotary evaporation. Ensuing acid chloride was redissolved in DMAc (30 mL) and used directly for further modification to model compound **2** using 0.006 mmol of phenol pursuing the above procedure (Scheme 3). Yield: 3.4706 g yellow powder, 96%; mp 362 °C; IR (KBr) ν_{max}: 3300–2500 (N–H, OH), 3042 (Ar C–H), 1695 (acid C=O), 1652 (amide C=O), 1602, 1515, 1450 (Ar C=C), 1231, 1206, 1036 (C–O), 834 (*p*-Ar), 746, 711 (monosubst Ar), 502. ^{1}H NMR (300 MHz, DMSO-d_6, ppm): δ 13.58 (s, 1H, COOH), 10.96 (s, 1H, amide NH), 10.81 (s, 1H, amide NH), 8.11 (d, 2H, J=5.3 Hz, *p*-Ar), 8.29 (d, 2H, J=5.2 Hz, *p*-Ar), 8.32 (d, 2H, J=5.4 Hz, *p*-Ar), 8.36 (d, 2H, J=5.6 Hz, *p*-Ar), 7–8 (m, 10H, Ar), 6.52 (s, 1H, pyrimidine), 6.68 (s, 1H, pyrimidine). ^{13}C NMR (75 MHz, DMSO-d_6, ppm): δ 176.32, 176.14 (acid C=O), 175.79, 175.52, 175.36 (ester C=O), 167.14, 166.98 (amide C=O), 162.84, 160.90, 157.15, 151.32, 149.46, 142.78, 135.23, 133.85, 131.64, 130.50, 129.28, 128.79, 127.68, 125.62, 121.11, 96.52, 96.46. Anal. Calcd for $C_{33}H_{22}N_4O_8$: C, 65.78; H, 3.68; N, 9.30%. Found: C, 65.75; H, 3.64; N, 9.27%.

4.3.4. Synthesis of model compound ***3***. A similar method for the synthesis of model compound **3** was followed, except that phenol (0.0011 g, 0.012 mmol) was used (Scheme 3). Yield: 3.950 g yellow powder, 97%; mp 358 °C; IR (KBr) ν_{max}: 3325 (amide N–H), 3046 (Ar C–H), 1652 (amide C=O), 1601, 1515, 1450 (Ar C=C), 1233, 1204, 1037 (C–O), 837 (*p*-Ar), 741, 712 (monosubst Ar), 501. ^{1}H NMR (300 MHz, DMSO-d_6, ppm): δ 10.91 (s, 1H, amide NH), 10.79 (s, 1H, amide NH), 8.32 (d, 4H, J=5.7 Hz, *p*-Ar), 8.40 (d, 4H, J=5.6 Hz, *p*-Ar), 7–8 (m, 15H, Ar), 6.90 (s, 1H, pyrimidine). ^{13}C NMR (75 MHz, DMSO-d_6, ppm): δ 175.20, 175.03, 174.89 (ester C=O), 166.85, 166.69 (amide C=O), 163.44, 161.20, 158.05, 152.42, 150.26, 145.38, 136.53, 133.95, 131.84, 130.70, 129.58, 128.89, 127.88, 125.92, 121.91, 91.25. Anal. Calcd for $C_{39}H_{26}N_4O_8$: C, 69.02; H, 3.86; N, 8.26%. Found: C, 68.97; H, 3.83; N, 8.22%.

Acknowledgements

S.S. gratefully acknowledges the Higher Education Commission of Pakistan (HEC) for fiscal assistance in this work under Indigenous 5000 PhD Fellowship Scheme Batch-II (042-111295-PS2-175).

Supplementary data

Supplementary data associated with this article can be found in the online version at doi:10.1016/j.tet.2010.06.065.

References and notes

1. Flory, P. J. *J. Am. Chem. Soc.* **1952**, *74*, 2718–2723.
2. Kim, Y. H.; Webster, O. W. *Polym. Prepr.* **1988**, *29*, 310–311.
3. Kim, Y. H.; Webster, O. W. *J. Am. Chem. Soc.* **1992**, *114*, 4947–4948.
4. Kim, Y. H.; Webster, O. W. *Macromolecules* **1992**, *25*, 5561–5572.
5. Fréchet, J. M. J.; Hawker, C. J.; Gitsov, I.; Leon, J. W. *J. Macromol. Sci., Pure Appl. Chem.* **1996**, *A33*, 1399–1425.
6. Malmstrom, E.; Hult, A. *J. Macromol. Sci., Rev. Macromol. Chem. Phys.* **1997**, *C37*, 555–579.
7. Kim, Y. H. *J. Polym. Sci., Part A: Polym. Chem.* **1998**, *36*, 1685–1698.
8. Fréchet, J. M. J. *Science* **1994**, *263*, 1710–1715.
9. Fréchet, J. M. J.; Henmi, M.; Gitsov, I.; Aoshima, S.; Grubbs, L. R. B. *Science* **1995**, *269*, 1080–1083.
10. Hawker, C. J.; Fréchet, J. M. J.; Grubbs, R. B.; Dao, J. *J. Am. Chem. Soc.* **1995**, *117*, 10763–10764.
11. Simon, P. F. W.; Radke, W.; Muller, A. H. E. *Macromol. Rapid Commun.* **1997**, *18*, 865–873.
12. De Brabander-van der Berg, E.; Meijer, E. *Angew. Chem., Int. Ed. Engl.* **1993**, *32*, 1308–1311.
13. Emrick, T.; Chang, H. T.; Fréchet, J. M. J. *Macromolecules* **1999**, *32*, 6380–6382.
14. Gaynor, S. G.; Edelman, S.; Matyjaszewsky, K. *Macromolecules* **1996**, *29*, 1079–1081.
15. Urich, K. E.; Hawker, C. J.; Fréchet, J. M. J.; Turner, S. R. *Macromolecules* **1992**, *25*, 4583–4587.
16. Turner, S. R.; Voit, B. I.; Mourey, T. H. *Macromolecules* **1993**, *26*, 4617–4623.
17. Yang, G.; Jikei, M.; Kakimoto, M. *Macromolecules* **1999**, *32*, 2215–2220.
18. Spindler, R.; Fréchet, J. M. J. *Macromolecules* **1993**, *26*, 4809–4813.
19. Fang, J. H.; Kita, H.; Okamoto, K. *Macromolecules* **2000**, *33*, 4639–4646.
20. Lin, Q.; Long, T. E. *Macromolecules* **2003**, *36*, 9809–9816.
21. Unal, S.; Yilgor, I.; Yilgor, E.; Sheth, J. P.; Wilkes, G. L.; Long, T. E. *Macromolecules* **2004**, *37*, 7081–7084.
22. Jikei, M.; Chon, S. H.; Kakimoto, M.; Kawauchi, S.; Imase, T.; Watanebe, J. *Macromolecules* **1999**, *32*, 2061–2064.
23. Hao, J. J.; Jikei, M.; Kakimoto, M. *Macromolecules* **2003**, *36*, 3519–3528.
24. Liu, Y.; Chung, T. S. *J. Polym. Sci., Part A: Polym. Chem.* **2002**, *40*, 4563–4569.
25. Gao, C.; Yan, D. Y. *Macromolecules* **2003**, *36*, 613–620.
26. Li, X. R.; Zhan, J.; Li, Y. S. *Macromolecules* **2004**, *37*, 7584–7594.
27. Fink, R.; Frenz, C.; Thelakkat, M.; Schmidt, H. W. *Macromolecules* **1997**, *30*, 8177–8181.
28. Saunders, J. H.; Frisch, K. C. *Polyurethanes: Chemistry and Technology*; Interscience: New York, NY, 1962; Vol. XVI, Parts I and II, pp 271–275.
29. Hawker, C. J.; Lee, R.; Fréchet, J. M. J. *J. Am. Chem. Soc.* **1991**, *113*, 4583–4588.
30. Jikei, M.; Kakimoto, M. *Prog. Polym. Sci.* **2001**, *26*, 1233–1285.
31. Li, X.; Lu, X.; Lin, Y.; Zhan, J.; Li, Y. g.; Liu, Z.; Chen, X.; Liu, S. *Macromolecules* **2006**, *39*, 7889–7899.